Article

Not peer-reviewed version

# Droplet-Based Microfluidic Photobioreactor (μ-PBR) as a Growth Optimization Tool for Cyanobacteria and Microalgae

Nadia Prasetija , Steffen Schneider , Ting Xie , Jialan Cao *

Posted Date: 11 October 2024

doi: 10.20944/preprints202410.0943.v1

Keywords: cyanobacteria; chlorella vulgaris; photobioreactor; droplet-based microfluidics; salt tolerance; dose-response screening; Synechococcus elongatus UTEX2973

*Article*

# Droplet-Based Microfluidic Photobioreactor as a Growth Optimization Tool for Cyanobacteria and Microalgae

**Nadia Prasetija [1,2], Steffen Schneider [1], Ting Xie [1] and Jialan Cao [1,*]**

[1] Technische Universität Ilmenau, Institute for Chemistry and Biotechnology, Dept. Physical Chemistry and Microreaction Technology, Weimarerstr. 32, D-98693 Ilmenau, Germany
[2] Institue for Bioprocess and Analytical Measurement Technology e.V., Rosenhof 37308 Heilbad Heiligenstadt
* Correspondence: Jialan.cao@tu-ilmenau.de

**Abstract:** Microalgae and cyanobacteria are photosynthetic microorganisms with significant biotechnological potential for the production of bioactive compounds, making them a promising resource for diverse industrial applications. This study presents the development and validation of a modular, droplet-based microfluidic photobioreactor (µPBR) designed for high-throughput screening and cultivation under controlled light conditions. The µPBR, based on polytetrafluoroethylene (PTFE) tubing and a 4-channel LED illumination system, enables precise modulation of light intensity, wavelength, and photoperiod, facilitating dose-response experiments. *Synechococcus elongatus* UTEX 2973 and *Chlorella vulgaris* were used to demonstrate the system's capacity to support photosynthetic growth under various conditions. The results indicate that continuous illumination, particularly under blue and mixed blue-red light, promotes higher autofluorescence and chlorophyll-a content in cyanobacteria *Synechococcus elongatus* UTEX2973, while *Chlorella vulgaris* achieved optimal growth under a 16:8 light-dark cycle with moderate light intensity. This µPBR offers not only a flexible, scalable platform for optimizing growth parameters but also investigating highly resolved dose response screenings of environmental stressors such as salinity. The findings highlight its potential for advancing microalgal biotechnology research and applications.

**Keywords:** cyanobacteria; *Chlorella vulgaris*; photobioreactor; droplet-based microfluidics; salt tolerance; dose-response screening; *Synechococcus elongatus UTEX2973*

## 1. Introduction

Eukaryotic microalgae and cyanobacteria are microscopic organisms that produce energy through oxygenic photosynthesis. They are widespread, found in nearly every habitat on Earth. AlgaeBase has documented over 50,000 species of living algae and 10,000 fossil species here referred to four kingdoms (Eubacteria, Chromista, Plantae, and Protozoa), 14 phyla, and 63 classes. They exhibit remarkable biological diversity with almost 6000 living species of cyanobacteria and more than 14000 living species of algae [1]. This diversity holds significant biotechnological potential for the production of valuable substances across various industries, such as feed, dietary supplements, pharmaceuticals, and the food industry.

The growth of photosynthetic microorganisms depends on numerous factors, including: 1) Light availability: Photosynthesis requires light as an energy source. Light encompasses not only duration and intensity but also wavelength, which can affect the growth of these microorganisms [2]. 2) Nutrients like carbon, nitrogen, phosphorus, and trace elements. 3) Temperature. 4) pH levels. 5) The salinity of the medium, as some species thrive better in saline environments than others. 6) Carbon

 doi:10.20944/preprints202410.0943.v1



dioxide concentration [3]. These factors work in combination, and changes in one or more can influence the growth and productivity of photosynthetic microorganisms.

The first cultivation of mono-algal cultures took place in 1890 with *Chlorella vulgaris*, with the study focusing on algal physiology [4]. Microalgae cultivation can be conducted in open systems (so-called "open ponds"). Shen et al. reported that there are three distinct open pond systems: raceway ponds, circular ponds, and unstirred ponds [5]. While these systems are cost-effective, they carry a high risk of contamination. The cultivation conditions are difficult to control, as they are heavily influenced by weather and climate. More recently, closed systems for the cultivation of microalgae have been developed for research and production purposes. Tubular reactors and flat-panel bioreactors are primarily used in research for the cultivation of cyanobacteria and microalgae [6,7].

Cyanobacteria are particularly attractive for their fast-photoautotrophic growth and the ability to be found in almost any place on the planet [8]. For many years, cyanobacteria have been studied for their biochemical properties, such as lipids, and pigments[8], as well as the production of carbohydrates, fatty acids, and alcohols as renewable sources of biofuels [9].

Over time, systems used for research and development have become smaller to conserve resources and increase efficiency. In recent years, droplet-based microfluidics has been increasingly studied. This technique applies the principles of conventional tubular bioreactors at the microliter scale and represents a promising alternative for media optimization and high-resolution dose-response screening [10]. Microfluidic photobioreactors are specialized systems that enable multiple experiments to be conducted simultaneously. They utilize microfluidic technologies to optimize the growth and cultivation of photosynthetic microorganisms, such as microalgae or cyanobacteria, in controlled environments. By employing microfluidics, these photobioreactors can precisely control the flow of nutrients, light, and other growth factors, leading to optimal growth or production of valuable bioactive compounds from photosynthetic microorganisms. This, in turn, can accelerate the research process [11,12].

*Microfluidic and Droplet-Based Microfluidic Photobioreactors*

Microfluidics deals with systems that handle or manipulate small volumes of fluid ($10^{-9}$ to $10^{-18}$ L) [13]. About 30 years ago, the first microfluidic devices were mainly aimed at miniaturizing analytical methods, especially to improve the separation of analytes [14]. Because of the small amount of fluid and, in many cases, system size, microfluidic systems have significant differences compared to conventional fluidic systems [15]. In the microscale, surface-bound effects are dominant, such as interfacial tension, electrostatic, and electrokinetic forces. In contrast, volume-bound effects such as inertia and gravity play a major role in the macroscale.

Microfluidics can be applied in numerous areas, for example, cell culture, drug research, separation processes, synthesis of nanomaterials, and diagnostics [15–17]. In cell culture, the miniaturized systems are a promising alternative for culturing photosynthetic microorganisms [10,11,18–21], tolerance determination against heavy metals [22,23], to organ-on-a-chip to investigate the pathophysiology of a disease and new therapeutic approaches [16,17].

Droplet-based microfluidics has been around since the early 1980s, but the number of examples of commercial applications is limited [24]. Droplet generation involves heterogeneous liquid-liquid systems, such as water/hexane and water/oil. Active control of droplet generation can be achieved by changing the flow rate or pressure of the liquid phases [25–30].

Key factors for microfluidic photobioreactor design include illumination, $CO_2$ supply, nutrient supply, and reactor mechanical form factors. Lighting parameters include intensity, wavelength, and temporal and spatial patterns. In addition, monitoring cell growth during cultivation and end-point detection of the desired product are also critical [18]. In the last decade, studies on droplet-based photobioreactors have been an attractive field of research. A lot of them were concentrated in chip-based microfluidic photobioreactors [11,12,19,20]. Cao et al. presented a droplet-based microfluidic platform that enables one-dimensional (1D) and two-dimensional (2D) screening of key parameters in cyanobacterial cultivation [10]. After generation, droplets containing cyanobacteria were stored in a PTFE microfluidic tube, cultivated under white fluorescence light, and growth was determined by

 doi:10.20944/preprints202410.0943.v1



photometric and fluorometric measurements. Subsequently, a high-throughput 1D screening of nitrate, phosphate, carbonate, and salt concentrations was performed.

In this contribution, we develop a high-throughput modular droplet-based µPBR with PTFE tubing as storage space, which will allow cultivation and dose-response screening under different light conditions. Moreover, the tubing is autoclavable, thereby it can be used multiple times. The µPBR was successfully validated by the growth of cyanobacteria and green algae *Chlorella vulgaris*.

## 2. Materials and Methods

### *2.1. Test Organisms and Chemicals*

For the experiments, a green microalga *Chlorella vulgaris* and a cyanobacterium strain *Synechococcus elongatus* UTEX 2973 (hereafter UTEX2973) were chosen. Both were cultivated in BG11 medium supplemented with 10 mM N-Tris(hydroxymethyl)methyl-2-aminoethanesulphonic acid buffer (MelFord, UK) to maintain a pH of 8.0. The composition of BG11 medium was as follow: 150 g/L $NaNO_3$ (VWR, Germany), 3.6 g/L $CaCl_2 \cdot 2\ H_2O$ (VWR, Germany), 0.6 g/L citric acid (VWR, Germany), 0.1 g/L EDTA (VWR, Germany), 7.5 g/L $MgSO_4 \cdot 7\ H_2O$ (VWR, Germany), 30.5 g/L $K_2HPO_4$ (Geyer, Germany), 20 g/L $Na_2CO_3$ (Merck, Germany), 2.86 g/L $H_3BO_3$ (Roth, Germany), 1.81 g/L $MnCl_2 \cdot 4\ H_2O$ (Merck, Germany), 0.222 g/L $ZnSO_4 \cdot 7\ H_2O$ (VWR, Germany), 0.39 g/L $Na_2MoO_4 \cdot 2\ H_2O$ (Applichem, Germany), 0.079 g/L $CuSO_4 \cdot 5\ H_2O$ (Merck, Germany), 0.049 g/L $Co(NO_3)_2 \cdot 6\ H_2O$ (Merck, Germany).

*Chlorella vulgaris* was sourced from the TU Karlsruhe, Institute of Applied Biosciences and Food Chemistry. The algae cells were pre-cultivated for 5 days at 25°C under constant shaking (100 rpm) and 16:8 h of light-dark cycle illumination provided by LED panel with white light with a color temperature of 4000K and an intensity of 3200 lumens (Delychi GmbH) until an optical density at 600 nm ($OD_{600}$) of 0.5 - 0.7 was reached. For the microfluid screening experiments, a cell suspension with a density of approximately $1x10^6$ cells/mL was used, resulting in an initial concentration of 500 cells within 500 nL/segment.

UTEX2973 was supplied by the working group for synthetic biology of photosynthetic organisms of the Friedrich-Schliller-University Jena. UTEX 2973 was grown in $BG11_{TES}$ medium. The pre-cultures for inoculation of the microfluidic experiments were grown in 100 ml Erlenmeyer flask filled with 20 mL $BG11_{TES}$ medium at 27°C with approximately continuous 75 µmol photon $m^{-2}\ s^{-1}$ white light for 3 to 4 days with $OD_{600}$ of 0.5 - 0.7. A cell suspension with a density of about $1x10^7$ cells/mL was applied for the microfluid screening experiments. Thus, the start concentration could be determined to be 5000 cells inside a 500 nL/segment.

As carrier phase, FLUTEC PP10 (F2 Chemicals, UK) was used for the experiments. For highly-resolved dose-response screening assay, a 0.6 M working solution of NaCl (VWR, Germany) was used.

### *2.2. The Development of Microfluid Photobioreactor*

The housing of our custom-developed microfluidic photobioreactor has dimensions comparable to a standard microtiter plate (127 mm × 86mm) and its components are shown in Figure 1. A µPBR consists of a 4-channel illumination unit (LEDs in an aluminum housing with cooling slots), onto which the fluid system to be illuminated (polytetrafluoroethylene, PTFE, tubing) is mounted. Two diffuser plates (2 mm and 3 mm) made of polycarbonate, with a gap of approximately 5 mm, ensure homogeneous light scattering (Figure 1 d). Three thin metal sheets separate the color channels. These sheets are placed directly between the LEDs on the LED array to prevent light contamination.

To control and determine light intensity of the individual LED arrays, a 2-in-1 spectro- and light meter, SpectraPen mini (Photon Systems Instruments, Czech Republic), was used. This device enables simultaneous spectral measurements of photon flux density (in µmol photon $m^{-2}\ s^{-1}$ or µE $m^{-2}\ s^{-1}$), irradiance in W $m^{-2}$, and illuminance in lux.

Preprints.org (www.preprints.org) | NOT PEER-REVIEWED | Posted: 11 October 2024 doi:10.20944/preprints202410.0943.v1



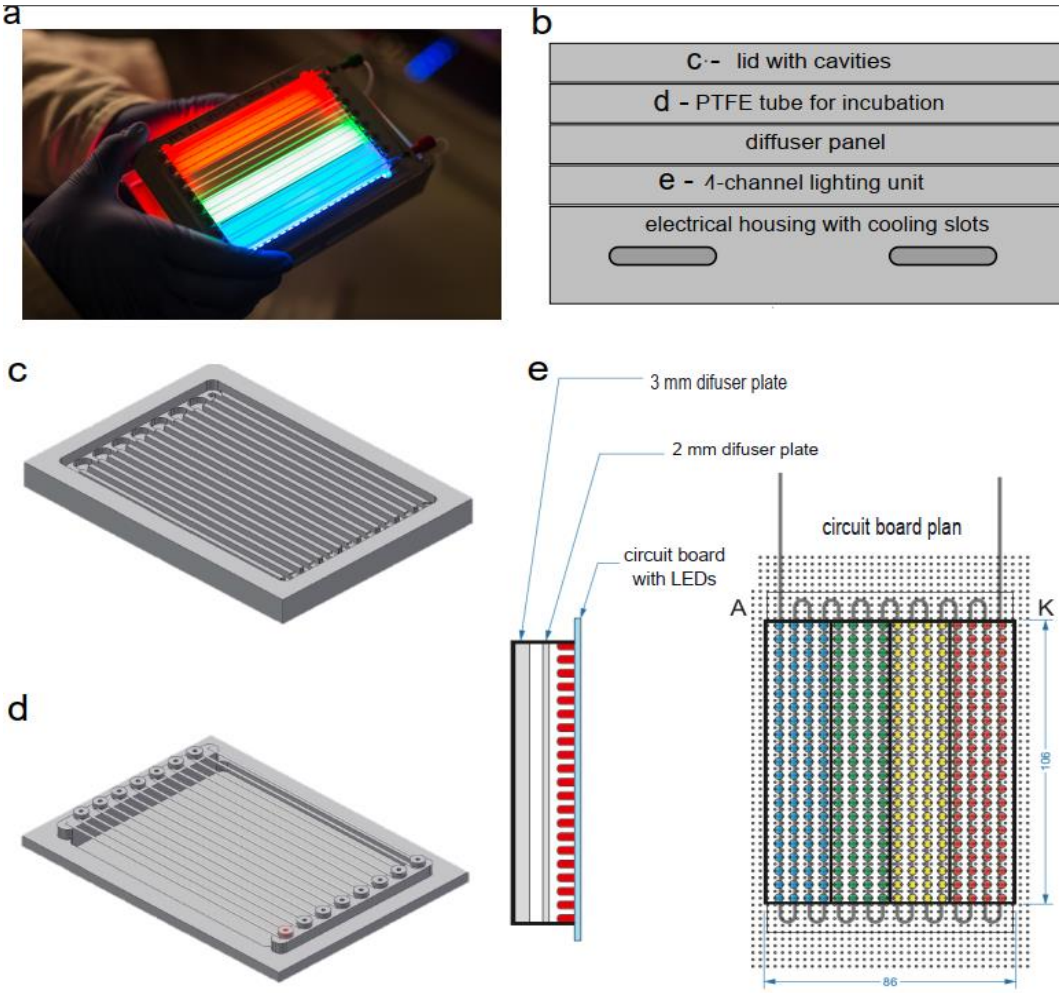


**Figure 1.** The detail construction of the µ-photobioreactor in microtiter plate format with an aluminum housing featuring cooling slots includes: (a) µ-photobioreactor in realization, (b) an overview, (C) an aluminum lid with machined cavities for 16 rows of tubing, preventing any light crosstalk between neighboring rows, (d) a holder for 2 meters of PTFE tubing for incubation and microscopy, and (e) the circuit board layout for the 4-block lighting unit and two diffuser plates (2 mm and 3 mm) made of polycarbonate, with a gap of approximately 5 mm, ensure homogeneous light scattering.

The meandered incubation tubing is made of PTFE with an inner diameter of 0.5 mm and an outer diameter of 1.0 mm (Figure 1 c). There are four rows of tubing in each color channel, providing a total of 16 rows of tubing in the µPBR. The system is closed with a lid made of aluminum with machined cavities for the tubing (Figure 1 b), ensuring that the individual rows are optically separated and can be individually illuminated. After generation, the droplets were stored and incubated in the µPBR.

For the growth experiments, 300 µmol photon $m^{-2}$ $s^{-1}$ was set, and by using printed filter foils, which had 0%, 20%, 50%, and 80% shading. The transmissions of the printed foils, which had 0%, 20%, 50%, and 80% shading, determined by the VIS spectrometer were 90%, 64%, 40%, and 18%, respectively, allowing photon flux densities of 270 µmol photon $m^{-2}$ $s^{-1}$, 192 µmol photon $m^{-2}$ $s^{-1}$, 120 µmol photon $m^{-2}$ $s^{-1}$, and 54 µE/$m^2$s to be adjusted. Four color blocks in combination with the printed foils allowed the simultaneous investigation of growth under 16 different growth conditions per µPBR. Dose-response screenings were conducted at a photon flux density of 120 µmol photon $m^{-2}$ $s^{-1}$.

 doi:10.20944/preprints202410.0943.v1



*2.3. Experimentals*

2.3.1. Microfluidic Cultivation Setup

For the experiment, the microfluidic segments were first generated (Figure 2). A multi-channel precision syringe pump system (Nemesys, CETONI GmbH) with up to five glass syringes was used for liquid dosing. The flow rate for each syringe could be individually adjusted via a computer program. One syringe was filled with the carrier medium Perfluoroperhydrofuran (FLUTEC PP10) as the separation phase unless otherwise specified. Three other syringes were then filled with the aqueous phases (medium, medium with cells, and medium with effector solution).

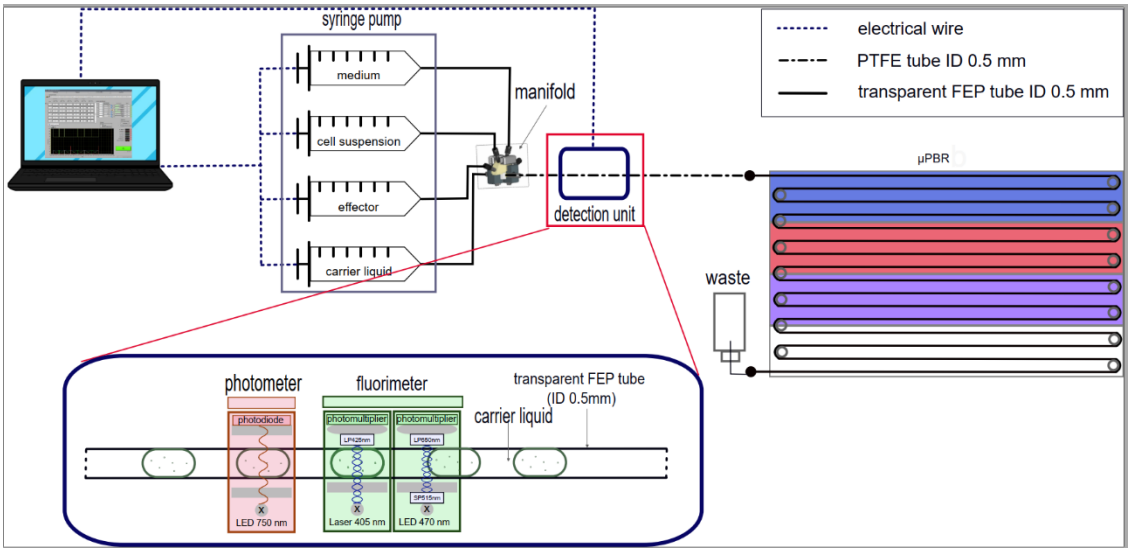


**Figure 2.** Droplet Generation Setup: computer-controlled syringe pump system with a 6-port manifold for droplet generation. The detection system: the aqueous segments (medium, effector, cells) separated by carrier liquid were pumped through a transparent FEP tube into a multi-channel detection unit for photometric and fluorometric measurements using a computer-controlled syringe pump system. The incubation tubing is made of PTFE with an inner diameter of 0.5 mm and an outer diameter of 1.0 mm. The length of the was 2.20 m. Approximately 28 droplets per row with a ca. 4 mm gap between droplets could be cultivated per run or up to 450 droplets.

All tubes connected to the individual syringes converge in a 6-way manifold, which mixes the aqueous phases and shapes them into microfluidic segments via a T-shaped channel structure. The segments were then directed to the detection system for the initial measurement. Afterward, they were routed into the incubation tubing of the µPBR. The manifold features a removable insert with various channel diameters. For the experiments, a PTFE insert with a 0.3 mm diameter for the vertical channel (inlet for the aqueous phase) and a 0.7 mm diameter for the horizontal channel (inlet for the carrier medium and outlet) was used [31]. For a tube with a 0.5 mm inner diameter and a flow rate ratio of approximately 2.1:1 (carrier medium 68 µL/min, aqueous phase 32 µL/min), a droplet volume of about 500 nL was generated. All tubes connected to the individual syringes and the incubation tubing are made of PTFE with an outer diameter of 1.0 mm and an inner diameter of 0.5 mm, except for the tube connected to the carrier medium syringe, which has an outer diameter of 1.6 mm and an inner diameter of 1.0 mm. A transparent fluorinated ethylene propylene (FEP) tube with an outer diameter of 1.6 mm and an inner diameter of 0.5 mm was used for the detection system.

The optical density at 750 nm ($OD_{750nm}$) was performed to monitor the growth of UTEX2973 and *Chlorella vulgaris*. On the excitation side, the fluorometric sensors consist of a laser diode or a power LED with a short-pass (SP) filter as the light source. On the detection side, a photomultiplier with a long-pass (LP) is installed.For an unspecific autofluorescence measurement, a 405 nm laser diode and a 425 nm LP emission filter were used. A 470 nm LED with a 515 nm SP filter as excitation and a 650 nm LP emission filter were used to detect chlorophyll a in the culture.

 doi:10.20944/preprints202410.0943.v1



2.3.2. Microfluid Screening Parameter

Both the cell concentration and the effector concentrations in the syringes must be twice as high as the desired maximum target concentration in the segment. As shown in Figure 3 a, the segment consists equally of cell suspension and medium/effector solution. For a dose-response screening of effectors, the cell concentration remains constant throughout the process, while the medium and effector concentrations change complementarily.

Figure 3 b shows a typical flow rate control program. The total flow rate is consistently 100 µL/min. The yellow curve represents the flow rate of the carrier medium FLUTEC PP10, which is 68 µL/min during segment generation. At the beginning, between segment sequences, and at the end, this flow rate is increased to 100 µL/min to maintain the overall flow rate. Blue represents the constant flow rate of the cell suspension at 16 µL/min. The medium and effector solution, shown in white and green respectively, have flow rates that change in opposite directions (16…0 µL/min and 0…16 µL/min). The short red bars of 2 seconds each correspond to the dye marking at the beginning and end of the segment sequences (approximately five segments each).

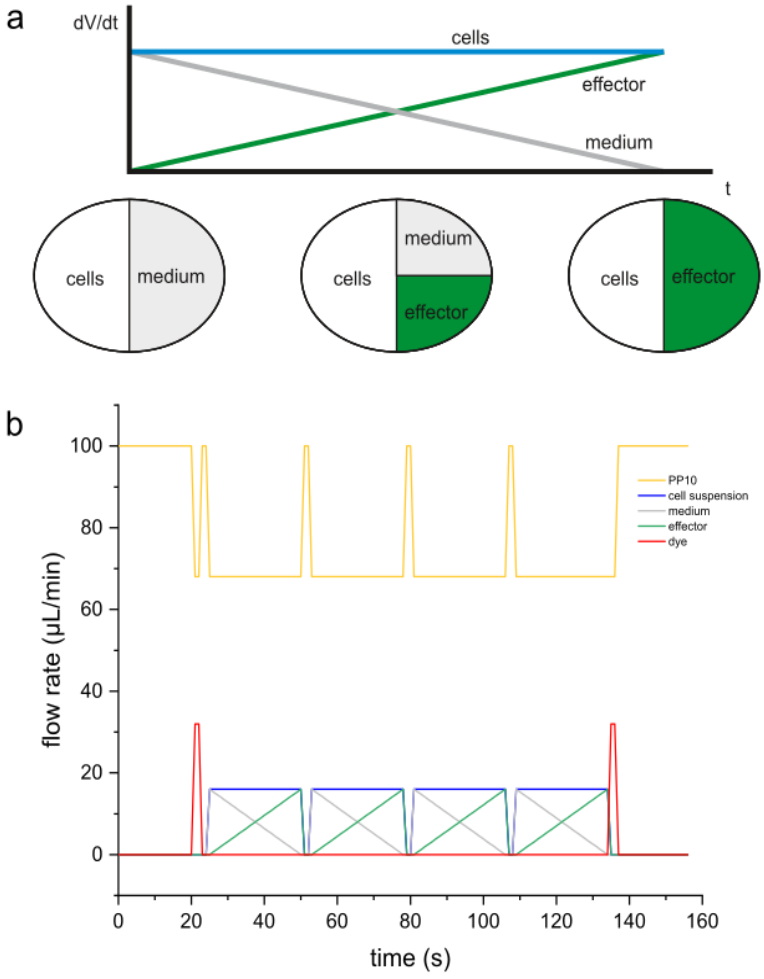


**Figure 3.** (a) Operation of the syringe pump system and composition of a segment in a dose-response screening and (b) syringe program for dose-response screening with four different illuminations.

2.3.3. Microflow-through Sensing and Data Processing

After droplet generation (time 0) and at the end of cultivation, the microfluidic segments were measured fluorometrically and photometrically using the microflow through detection unit (Figure 2). For droplet sequence quality control, photometric measurements were taken at 470 nm,

 doi:10.20944/preprints202410.0943.v1



and optical density at 750 nm ($OD_{750nm}$) was measured to monitor the growth of UTEX2973 and *Chlorella vulgaris*. Two fluorometric sensors are integrated into the detection system. For non-specific autofluorescence measurement, a 405 nm laser diode and a 425 nm LP emission filter were used. To detect chlorophyll a in the culture, a 470 nm LED with a 515 nm SP filter for excitation and a 650 nm LP emission filter were used.

The measured raw data from the multi-channel sensors were processed and analyzed using an LabView evaluation program. Segments incubated in the non-irradiated tubing areas at the end of each row (180° bends) were cut out. The area to be cut out could be dynamically adjusted and was approximately 20–25%.

In pharmacology and toxicology, the median effective concentration ($EC_{50}$) is specified, where a half-maximal effect is observed. The $EC_{50}$ value must be derived from a specific dose-response curve, typically a sigmoidal function, through mathematical modeling, corresponding to the inflection point of the fitted curve. Numerous model functions are available to fit dose-response curves. One of the most well-known models is the Hill equation, which was also used in this work:

$$\frac{E}{E_{max}} = \frac{[A]^n}{EC_{50}^n + [A]^n} = \frac{1}{1 + \left(\frac{EC_{50}}{[A]}\right)^n}$$

where E is the extent of the response, [A] is the concentration of the drug or effector, $EC_{50}$ is the effector concentration that produces a 50% maximal response, and n is the Hill coefficient.

## 3. Results and Discussion

### *3.1. Microfluid Photo Bioreactor Characterization*

The temperature was strongly influenced by the wavelengths used and the set intensity. The optimal cultivation temperature for the model organisms is between 28 and 41°C [32,33]. For the entire study, light intensities were set to 120 µmol photon $m^{-2}$ $s^{-1}$ for dose-response screening and 300 µmol photon $m^{-2}$ $s^{-1}$ for growth examination. The temperature was measured every 24 hours until the end of cultivation to monitor its stability.

Figure 4 shows the temperature development for white LEDs (color temperature of 4000K), blue (470 nm), red (660 nm), and blue-red mixed (470 nm + 660 nm) LED strips in dependence of the light intensity. At the lower light intensity of 120 µmol photon $m^{-2}$ $s^{-1}$, all these selected wavelengths show that the temperature stabilized at around 26–28°C after 70 minutes (Figure 4 a). At the higher light intensity of 300 µmol photon $m^{-2}$ $s^{-1}$, the temperature stabilized after 100 minutes, peaking at around 32°C (Figure 4 b). It could be observed that the mixed-light and white LEDs have a slightly higher average temperature than blue and red LEDs.

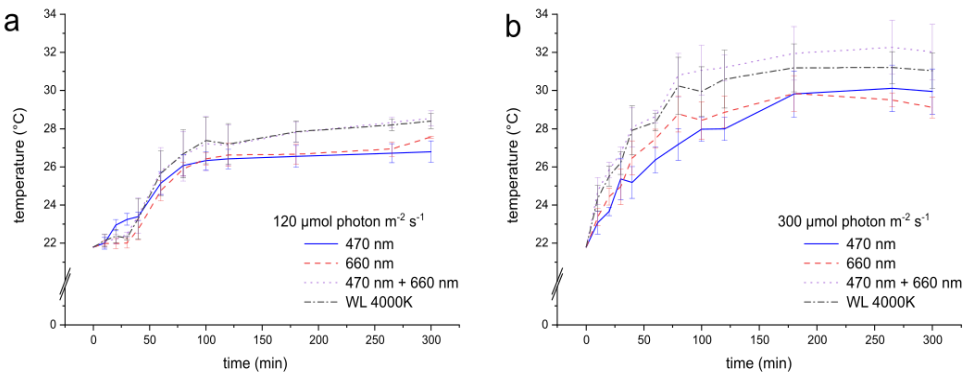


**Figure 4.** Temperature development of the light system at 120 µmol photon $m^{-2}$ $s^{-1}$ (a) and 300 µmol photon $m^{-2}$ $s^{-1}$ (b) up to 300 minutes. n = 6 and error bars represent the standard deviation.

Longtime experiments until 7 days show the temperatures remained stable at both 120 µmol photon $m^{-2}$ $s^{-1}$ and 300 µmol photon $m^{-2}$ $s^{-1}$. Throughout the experiment, the temperature remained in the range of 28 ± 0.5°C at 120 µmol photon $m^{-2}$ $s^{-1}$ and around 32 ± 0.5°C at 300 µmol photon $m^{-2}$ $s^{-1}$.

 doi:10.20944/preprints202410.0943.v1



Overall, it can be concluded that with this setup, the temperature across all tested wavelengths remained constant after 2 hours.

*3.2. Influence of Different Light Condition of Green Algae Chlorella vulgaris Growth*

For the experiment, the following LED strips were used: white light with a color temperature of 4000K (WL4000K), blue light at 470 nm, red light at 660 nm, and mixed LEDs (470 nm + 660 nm). The set illuminance for all colors was 300 µmol photon $m^{-2}$ $s^{-1}$. Using a printed film with varying degrees of blackening at 0%, 20%, 50%, and 80%, the transmission values corresponded to 90%, 64%, 40%, and 18% of the set illuminance. The light intensities for the respective colors were thus 270 µmol photon $m^{-2}$ $s^{-1}$, 192 µE/$m^2$s, 120 µmol photon $m^{-2}$ $s^{-1}$, and 54 µmol photon $m^{-2}$ $s^{-1}$. Two lighting modes were employed for cultivation: 1) a 16:8 light-dark cycle and 2) continuous illumination.

The growth of *Chlorella vulgaris* was cultivated under the above-mentioned light conditions (Figure 5). The culture was measured both photometrically and fluorometrically on the sixth day of cultivation. The optical density at 750 nm ($OD_{750nm}$) was used as one of the growth parameters. The non-specific and chlorophyll a (Chl a) autofluorescence intensity were also measured. Non-specific autofluorescence was measured using a 405 nm laser diode and a 425 nm LP emission filter. For the detection of Chl a, a 470 nm with a 515 nm SP filter as excitation and a 650 nm LP emission filter were used.

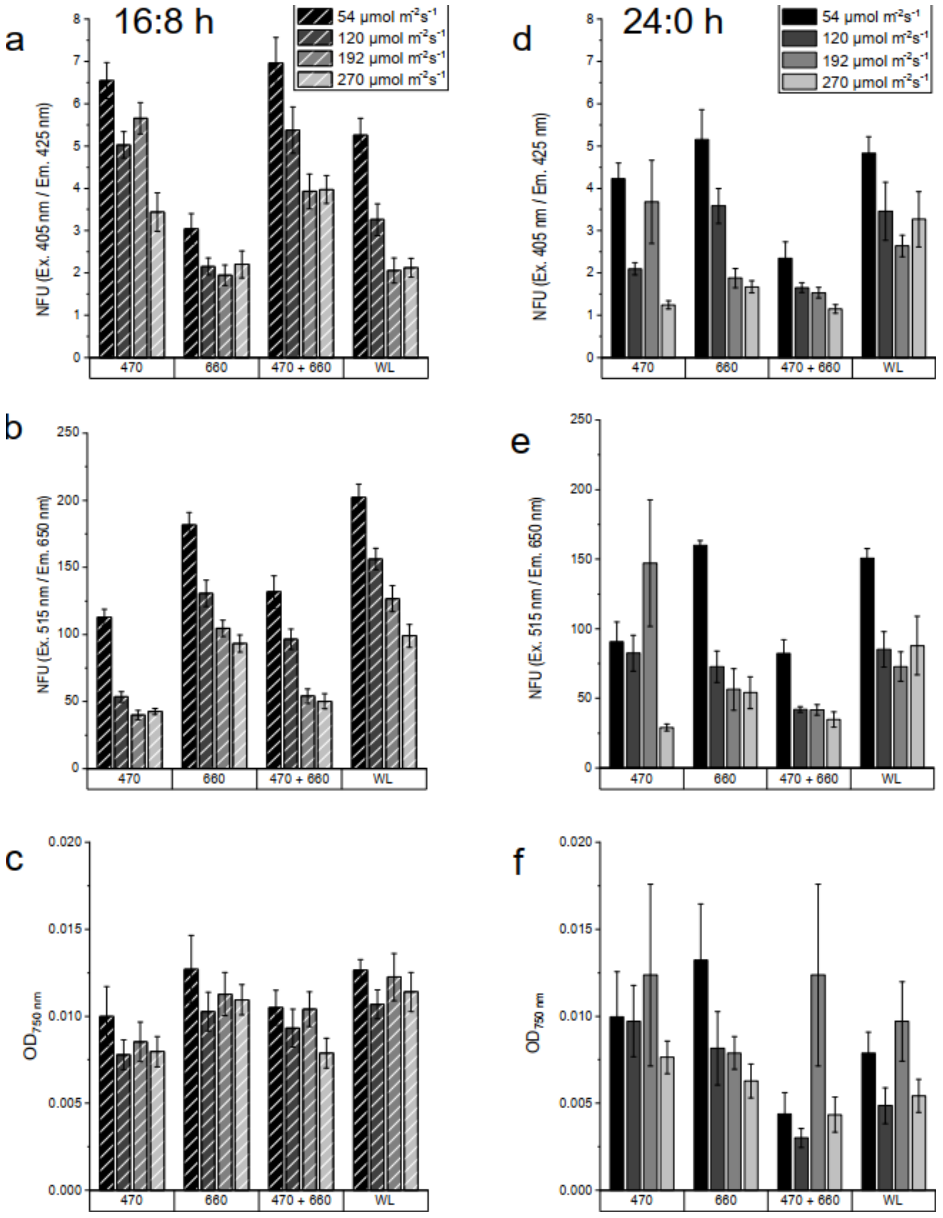

 doi:10.20944/preprints202410.0943.v1



**Figure 5.** *Chlorella vulgaris* in BG11 medium on the 6th day of cultivation in 500 nL droplets. The droplets were cultivated with three different wavelengths (470 nm, 660 nm, mix 470 nm + 660 nm) and a white light (4000K) and lighting modes 16:8 light-dark cycle (fig. a-c) and continuous illumination (fig. d-f). For the data evaluation, non-specific autofluorescence was measured using a 405 nm laser diode and a 425 nm LP emission filter (fig.a, d). For the detection of Chl a, a 470 nm excitation with a 515 nm SP filter and a 650 nm LP emission filter were used (fig. b,e). Optical density at 750 nm was used as growth parameters (fig. c and f).

The culture was measured both photometrically and fluorometrically on the sixth day of cultivation. Figure 5 shows (a) (d) the non-specific autofluorescence intensity, (b) (e) the Chl a, and (c) (f) the optical density at 750 nm at 16:8 light-dark cycle (a,b,c) and continuous illumination (d,e,f). In general, *Chlorella* growing under 16:8 light and dark cycles showed less dispersion than in the 24:0 without synchronization phases and the values of all growth parameters were higher in the 16:8 light cycle compared to the continuously illuminated cultures. Both non-specific and Chl a autofluorescence intensity measurements yielded similar results. The values decreased with increasing light intensity. The highest values measured by Chl a autofluorescence intensity were shown by the lowest intensity at 54 µmol photon $m^{-2}$ $s^{-1}$ of WL 4000K and 660 nm with 16:8 light cycle (Figure 5b). Chl a autofluorescence intensity under continuous illumination with 470 nm at 192 µmol photon $m^{-2}$ $s^{-1}$ showed high intensity with strong variations. All illumination colors under 16:8 illumination cycle showed no significant differences values while under continuous exposure shows a great variance in $OD_{750nm}$.

Optimal biomass and pigment production in *Chlorella vulgaris* can be targeted by optimizing the light conditions. The light cycle, choice of wavelength, and light intensity are all taken into account. *Chlorella vulgaris* is best suited with a 16:8 light cycle at 100 µmol photon $m^{-2}$ $s^{-1}$, where it reached the highest final cell number up to 90-fold initial cell number [3]. Increasing light intensity has also been reported to alter pigment composition. Increasing light intensity decreases chlorophyll concentration but induces carotenoid production in microalgae [2,3,34,35]. It could be that the pigment changes are an adaptation mechanism to the strong light. Low light induced the synthesis of larger photosynthetic units, presumably to support light uptake, while in high light, smaller photosynthetic units were synthesized, presumably to avoid light damage. There was also a significant decrease in Chl a content with increasing light intensity, which could not be promoted by faster growth pigment accumulation [3]. Thus, the studies are consistent with the Chl a and non-specific autofluorescence intensities in this experiment, in which autofluorescence intensities decreased with increasing light intensity.

### *3.3. Influence of Different Light Condition of Cyanobacteria UTEX2973 Growth*

For the experiment, the following LED strips were used: white light with a color temperature of 4000K (WL4000K), blue light at 470 nm, red light at 660 nm, and mixed LEDs (470 nm + 660 nm). The light intensities for the respective colors were thus 270 µmol photon $m^{-2}$ $s^{-1}$, 192 µmol photon $m^{-2}$ $s^{-1}$, 120 µmol photon $m^{-2}$ $s^{-1}$, and 54 µmol photon $m^{-2}$ $s^{-1}$. Two lighting modes were employed for cultivation: 1) a 16:8 light-dark cycle and 2) continuous illumination. As results, Figure 6 show the microscopic representation of UTEX2973 in BG11 medium on the 6th day of cultivation with 200X magnification. Obviously, under 16:8 light-dark cycle (Figure 6 a,b,c,d) show much lower cell density compared to 24:0 illumination ((Figure 6 e,f,g,h).

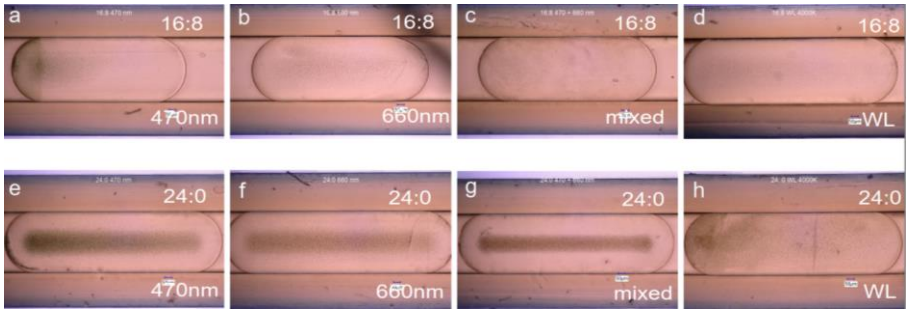

 doi:10.20944/preprints202410.0943.v1



**Figure 6.** Microscopic representation of UTEX2973 in BG11 medium on the 6th day of cultivation with 200X magnification. The droplets were cultivated different wavelengths at 470 nm (a,e), 660 nm (b,f), mix 470 nm + 660 nm (c,g) and a white light 4000K (d,h). Two lighting modes were employed for cultivation: (a,b,c,d) 16:8 light-dark cycle, (e,f,g,h) continuous illumination.

The culture was measured both photometrically and fluorometrically on the sixth day of cultivation. Figure 7 shows (a) (d) the non-specific autofluorescence intensity, (b) (e) the Chl a, and (c) (f) the optical density at 750 nm at 16:8 light-dark cycle (left) and continuous illumination (right). Generally, the values of all growth parameters were higher in cultures under continuous illumination compared to the 16:8 light-dark cycle and decreased slightly with increasing light intensity. The highest autofluorescence intensities, both Chl a and non-specific, were observed in the culture continuously incubated under blue light at the lowest intensity (54 µmol photon $m^{-2}$ $s^{-1}$), while the maxima biomass was observed under mixed and white light at 54 µmol photon $m^{-2}$ $s^{-1}$. Under the same conditions but with a 16:8 light-dark cycle, the autofluorescence intensity was approximately 40% lower compared to continuous illumination. Figures 7 b and e clearly show that the UTEX2943 cultures underWL 4000K, 660 nm, and 470 nm + 660 nm provided almost identical Chl a content, and generally, the Chl a content decreased with increasing light intensity.

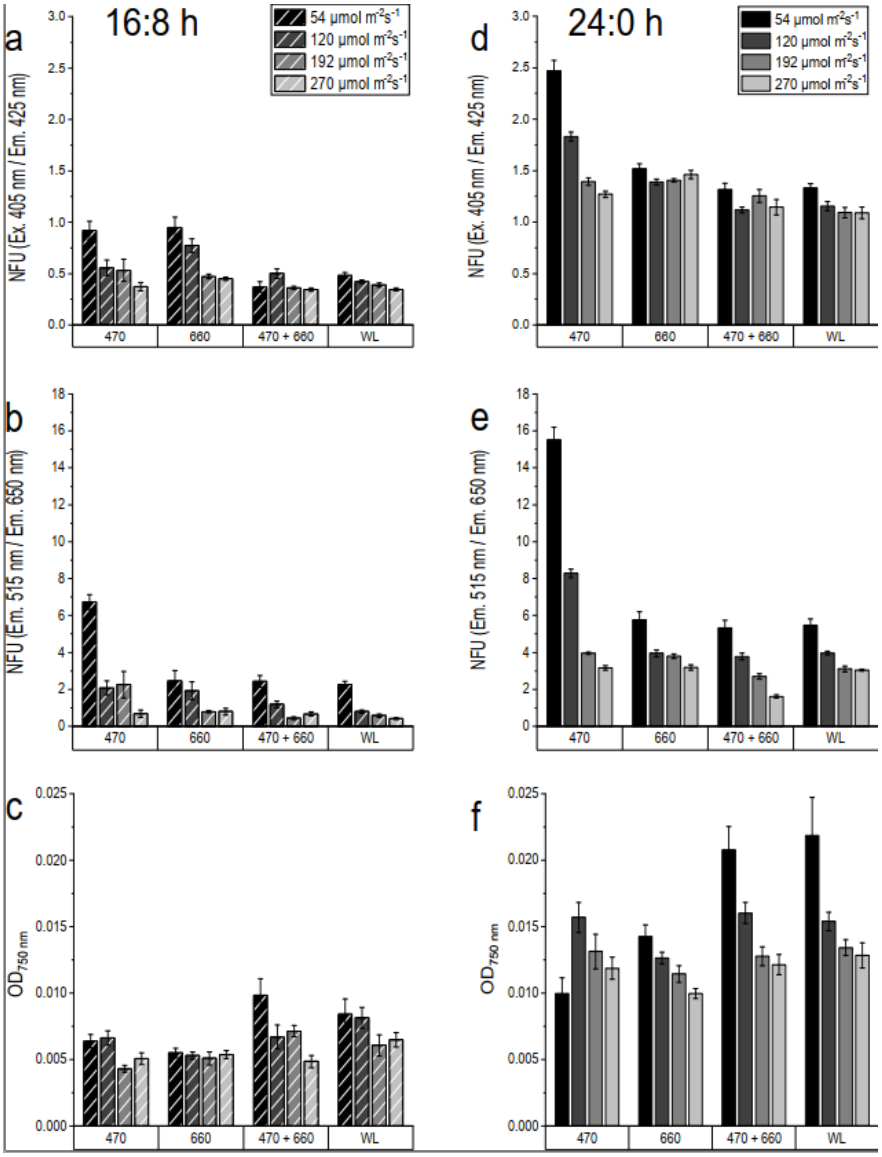


**Figure 7.** Multiparameter determination of the growth of UTEX2973 in BG11 medium on the 6th day of cultivation in 500 nL droplets. The droplets were cultivated with three different wavelengths (470 nm, 660 nm, mix 470 nm + 660 nm) and a white light (4000K) and lighting modes 16:8 light-dark cycle

 doi:10.20944/preprints202410.0943.v1



(a-c) and continuous illumination (d-f). For the data evaluation, non-specific autofluorescence was measured using a 405 nm laser diode and a 425 nm LP emission filter (a, b). For the detection of Chl a, a 470 nm excitation with a 515 nm SP filter and a 650 nm LP emission filter were used (c,d). Optical density at 750 nm was used as a growth parameters (d,f).

Cyanobacteria can grow at very high light intensities, but higher light intensity leads to a decrease in the surface density of thylakoid membranes and Chl a content, which was also confirmed by our study. The absorption of specific wavelengths of light causes a modification in their pigment composition. The change in pigment is directly related to the ability to adapt to different light intensities and durations. An increased content of phycocyanin was observed when a cyanobacterial strain, *Calothrix sp.* PCC7601, was cultured under red light [36]. This explains why the results of the autofluorescence intensity measurements differed somewhat.

The non-specific autofluorescence intensity measurement included all other pigments such as phycoerythrin (PE) and phycocyanin (PC), whereas the other autofluorescence intensity sensor measured only the Chl a content. The cultures irradiated with continuous blue light showed similar changes in non-specific and Chl a autofluorescence intensities. This indicates that with increasing blue light intensity, the pigment composition in the cells decreased proportionally. While the Chl a content decreased under continuous 660 nm and mixed 470 nm + 660 nm, other pigments increased. Similar results were reported in a study [37] that investigated the Chl a autofluorescence intensity of a cyanobacterial strain, *Synechocystis sp.* PCC6803, cultured under blue light (450 nm) and red light (660 nm) at various intensities. An increase in blue light intensity reduced both Chl a and PC autofluorescence intensity. An increase in Chl a autofluorescence intensity was observed with increasing red-light intensity, while the autofluorescence intensity decreased.

$OD_{750nm}$ measurements showed no significant differences between 470 nm and 660 nm at all intensities. The highest values were observed in cultures continuously illuminated under 54 µmol photon $m^{-2}$ $s^{-1}$WL 4000K and 470 nm + 660 nm, which decreased with increasing light intensity (Figure 6 c and f). In a 16:8 light cycle, the 470 nm + 660 nm cultures showed the highest values at all intensities, while they showed the lowest values under red light, and different light intensities had no effect on cell density. The $OD_{750nm}$ value correlated closely with cell number but did not allow differentiation between living and dead cells. On the other hand, growth could be determined by measuring endogenous cellular autofluorescence intensity, which allowed an estimation of the approximate number of physiologically active cells [10]. Although the culture under 54 µmol photon $m^{-2}$ $s^{-1}$ continuous 470 nm showed the highest autofluorescence intensities, its $OD_{750nm}$ was only half that of 470 nm + 660 nm. This could indicate that the cells cultured under 470 nm were packed with a higher pigment content.

Overall, growth determination using multi-parameter sensors enables the optimization of targeted value-added production in cyanobacteria. For example, to achieve higher chlorophyll yields, UTEX2973 can be cultured under 54 µmol photon $m^{-2}$ $s^{-1}$ continuous illumination under 470 nm. If biomass production is the goal, it grows best under 54 µmol photon $m^{-2}$ $s^{-1}$ continuous illuminationWL 4000K or combined light with 470 nm and 660 nm.

### *3.4. Realization of the Combinatorial Effect of Dose-Response Experiment with NaCl under Various Light Condition*

Cyanobacteria pursue limited sodium uptake and release via the $Na^+/H^+$ antiport as a control mechanism in the accumulation of elevated $Na^+$ ions in the cytoplasm. Although higher inorganic ion concentrations can damage the cell growth and metabolism of cyanobacteria, they are much more resistant to salt stress compared to higher plants [38]. In this experiment, the influence of different wavelengths of irradiated cultivation light on the salt tolerance of UTEX2973 was investigated.

UTEX2973 was cultured for dose-response screening against NaCl under white light with a color temperature of 4000K (WL4000K), red light 660 nm, blue light at 470 nm and a mixed blue and red light (470 nm + 660 nm) at 120 µmol photon $m^{-2}$ $s^{-1}$ (Figure 8). The NaCl concentration was 0-0.6 M. Previously, it was confirmed that UTEX2973 grows best under continuous illumination. For this

 doi:10.20944/preprints202410.0943.v1



experiment, the culture was therefore incubated under continuous illumination. The unspecific autofluorescence intensity of the culture was measured on the sixth day of cultivation using microflow fluorometry with a 405 nm laser diode and an LP emission filter of 425 nm.

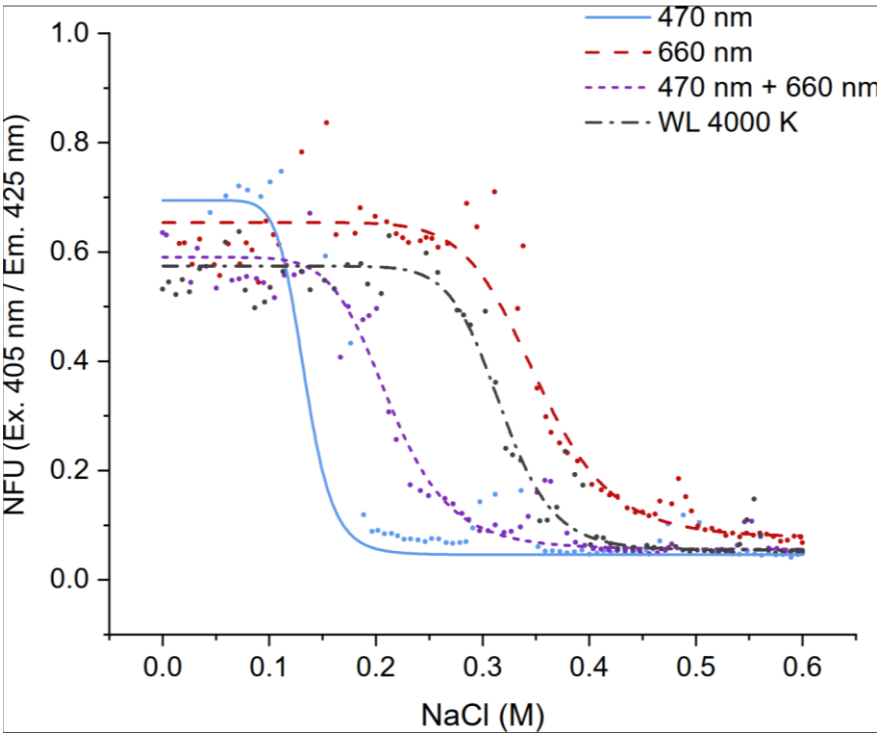


**Figure 8.** Dose-response curves of UTEX2973 against NaCl (0 - 0.6 M). The cultures were measured on the sixth day of cultivation in 500 nL droplets. The cultivation temperature was 32 ± 0.5 °C. The unspecific autofluorescence measurement was performed with a 405 nm laser diode and an LP emission filter of 425 nm. The droplets were cultivated with three different wavelengths (470 nm, 660 nm, mix 470 nm + 660 nm) and a white light (WL 4000K) with continuous illumination.

Under white and red-light exposure, the $EC_{50}$ values were approx. 0.35 ± 0.03 M NaCl. Comparatively, the salt tolerance of UTEX2973 decreased significantly under blue light ($EC_{50}$ blue = 0.13 M NaCl). $EC_{50}$ of blue and red mixed light (470 nm + 660 nm) was 0.21 M NaCl and thus exactly in the middle between 470 nm and 660 nm. Overall, this confirmed the findings from our previously research which showed that *Synechococcus elongatus* UTEX2973 decreased biomass from 0.3 M NaCl and an $EC_{50}$ value of about 0.4 M NaCl [10]. Model organisms *Synechococcus sp* UTEX3154 and *Synechocystis sp.* PCC6803 have a higher salt tolerance of about 0.85 M and up to 1.2 M NaCl [2,10,38].

It was also observed that in the sublethal concentration range between 0.3 - 0.38 M NaCl of 470 nm, 0.45 - 0.5 M NaCl of 470 nm + 660 nm and 660 nm, there was an increased autofluorescence intensity. This phenomenon can be explained by the fact that high salinity inhibits the growth and photosynthesis of cyanobacteria, but also induces some specific salt stress proteins and increases cell chlorophyll content [38]. Overall, the 1D screening data confirmed that our microfluidic platform is well-suited for investigating the cyanobacterial response to individual effectors. This example clearly demonstrates that the illumination wavelength plays a significant role in the salt tolerance of cyanobacteria UTEX2973.

## 4. Conclusions and Outlook

Our study demonstrates the successful application of a droplet-based microfluidic photobioreactor (µPBR) for high-throughput cultivation and screening of photosynthetic microorganisms. The modular design of the µPBR allows precise control over light conditions and facilitates multiple parallel experiments, providing an innovative tool for optimizing the growth of microalgae and cyanobacteria. The ability to vary light conditions and conduct dose-response

 doi:10.20944/preprints202410.0943.v1



screenings highlights the system's utility in investigating environmental influences on photosynthetic efficiency and bioactive compound production.

Future work could expand the capabilities of the µPBR by incorporating additional environmental parameters such as temperature and gas content, further increasing its versatility. This platform also shows promise for industrial applications, where rapid optimization of cultivation conditions is critical for maximizing biomass production and compound yields. With the integration of advanced sensing technologies and automation, the µPBR could be scaled for larger bioprocesses, contributing to the sustainable production of biofuels, pharmaceuticals, and other valuable bioproducts. The next steps in this research will focus on optimizing the system for specific industrial strains and exploring its applicability to other biotechnologically relevant organisms.

**Supplementary Materials:** The following supporting information can be downloaded at the website of this paper posted on Preprints.org.

**Author Contributions:** Laboratory measurements and data analysis, N.P. T.X. and S.S.; conceptualization and writing—original draft preparation, J.C. and N.P.; writing-review and editing, J.C., N.P. and S.S. All authors have read and agreed to the published version of the manuscript.

**Funding:** J.C. gratefully acknowledges the financial support provided by a habilitation scholarship from the Technische Universität Ilmenau. T.X. is grateful for a scholarship from Landesgraduiertenförderung Thuringia.

**Data Availability Statement:** All cyanobacterial strains used in this study are available for purchase from the Pasteur Culture Collection, Paris (France) or the UTEX Culture Collection of Algae, University of Texas, Austin (USA). The processed raw data of all experiments are provided in the Supplementary Data files.

**Acknowledgments:** We would like to express our gratitude to Jun. Prof. Julie Zedler from the Friedrich Schiller University Jena, Matthias Schleiden Institute for Genetics, Bioinformatics, and Molecular Botany, Synthetic Biology of Photosynthetic Organisms, for providing us with the cyano strains. We also thank Christian Steinweg from the TU Karlsruhe, Institute of Applied Biosciences of Food Chemistry, for supplying *Chlorella vulgaris*. Our thanks extend to the faculty workshop for realizing the microfluidic photobioreactor, and to Frances Möller for her assistance in the lab.

**Conflicts of Interest:** The authors declare no conflicts of interest.

## References

1. Guiry, M. How many species of algae are ther? *J.Phycol.* **2012**, 1057–1063, doi:10.1111/j.1529-8817.2012.01222.x.
2. EL-Sheekh, M.M.; Dewidar, S.; Hamad, A. The Influence of Different Light Wavelengths on Growth, Enzymes Activity and Photosynthesis of the Marine Microalga Dunaliella parva W.Lerche 1937. *Baghdad Sci.J* **2021**, *18*, 268, doi:10.21123/bsj.2021.18.2.0268.
3. Seyfabadi, J.; Ramezanpour, Z.; Amini Khoeyi, Z. Protein, fatty acid, and pigment content of *Chlorella vulgaris* under different light regimes. *J Appl Phycol* **2011**, *23*, 721–726, doi:10.1007/s10811-010-9569-8.
4. Ahmad, I.; Abdullah, N.; Koji, I.; Yuzir, A.; Eva Muhammad, S. Evolution of Photobioreactors: A Review based on Microalgal Perspective. *IOP Conf. Ser.: Mater. Sci. Eng.* **2021**, *1142*, 12004, doi:10.1088/1757-899X/1142/1/012004.
5. Shen, Y.; Yuan, W.; Pei, Z.J.; Wu, Q.; Mao, E. Microalgae Mass Production Methods. *Transactions of the ASABE* **2009**, *52*, 1275–1287, doi:10.13031/2013.27771.
6. Jodlbauer, J.; Rohr, T.; Spadiut, O.; Mihovilovic, M.D.; Rudroff, F. Biocatalysis in Green and Blue: Cyanobacteria. *Trends Biotechnol.* **2021**, *39*, 875–889, doi:10.1016/j.tibtech.2020.12.009.
7. Ardiansyah, S.R.; Orlando, A.M.; Rahman, A.; Prihantini, N.B.; Nasruddin. Tubular Photobioreactor: A Preliminary Experiment Using Synechococcus sp. (Cyanobacteria) Cultivated in NPK Media for Biomass Production as Biofuel Feedstock. *Evergreen* **2019**, *6*, 157–161, doi:10.5109/2321011.

8. *The pharmacological potential of cyanobacteria*: *Trends in Cyanobacteria: a contribution to systematics and biodiversity studies*. Chapter 1; Hentschke, G.S.; Gama Jr., W.A., Eds.; Academic Press: London, United Kingdom, San Diego, CA, United States, 2022, ISBN 978-0-12-821491-6.
9. Aboim, J.B.; Oliveira, D.T. de; Mescouto, V.A. de; Dos Reis, A.S.; Da Rocha Filho, G.N.; Santos, A.V.; Xavier, L.P.; Santos, A.S.; Gonçalves, E.C.; do Nascimento, L.A. Optimization of Light Intensity and NaNO3 Concentration in Amazon Cyanobacteria Cultivation to Produce Biodiesel. *Molecules* **2019**, *24*, doi:10.3390/molecules24122326.
10. Cao, J.; Russo, D.A.; Xie, T.; Groß, G.A.; Zedler, J.A.Z. A droplet-based microfluidic platform enables high-throughput combinatorial optimization of cyanobacterial cultivation. *Sci. Rep.* **2022**, *12*, 15536, doi:10.1038/s41598-022-19773-6.
11. Kim, H.; Weiss, T.L.; Thapa, H.R.; Devarenne, T.P.; Han, A. A microfluidic photobioreactor array demonstrating high-throughput screening for microalgal oil production. *Lab Chip* **2014**, *14*, 1415–1425, doi:10.1039/c3lc51396c.
12. Perin, G.; Cimetta, E.; Monetti, F.; Morosinotto, T.; Bezzo, F. Novel micro-photobioreactor design and monitoring method for assessing microalgae response to light intensity. *Algal Res.* **2016**, *19*, 69–76, doi:10.1016/j.algal.2016.07.015.
13. Whitesides, G.M. The origins and the future of microfluidics. *Nature* **2006**, *442*, 368–373, doi:10.1038/nature05058.
14. Berlanda, S.F.; Breitfeld, M.; Dietsche, C.L.; Dittrich, P.S. Recent Advances in Microfluidic Technology for Bioanalysis and Diagnostics. *Anal. Chem.* **2021**, *93*, 311–331, doi:10.1021/acs.analchem.0c04366.
15. Nguyen, N. *Mikrofluidik: Entwurf, Herstellung und Charakterisierung;* B.G. Teubner Verlag/GWV Fachverlage GmbH: Wiesbaden, 2004.
16. Niculescu, A.; Chircov, C.; Bîrcă, A.C.; Grumezescu, A.M. Fabrication and Applications of Microfluidic Devices: A Review. *Int. J. Mol. Sci.* **2021**, *22*, doi:10.3390/ijms22042011.
17. Gharib, G.; Bütün, I.; Muganlı, Z.; Kozalak, G.; Namlı, I.; Sarraf, S.S.; Ahmadi, V.E.; Toyran, E.; van Wijnen, A.J.; Koşar, A. Biomedical Applications of Microfluidic Devices: A Review. *Biosensors (Basel)* **2022**, *12*, doi:10.3390/bios12111023.
18. Yang, Y.; Wang, C. Review of Microfluidic Photobioreactor Technology for Metabolic Engineering and Synthetic Biology of Cyanobacteria and Microalgae. *Micromachines (Basel)* **2016**, *7*, doi:10.3390/mi7100185.
19. Castaldello, C.; Sforza, E.; Cimetta, E.; Morosinotto, T.; Bezzo, F. Microfluidic Platform for Microalgae Cultivation under Non-limiting CO 2 Conditions. *Ind. Eng. Chem. Res.* **2019**, *58*, 18036–18045, doi:10.1021/acs.iecr.9b02888.
20. Westerwalbesloh, C.; Brehl, C.; Weber, S.; Probst, C.; Widzgowski, J.; Grünberger, A.; Pfaff, C.; Nedbal, L.; Kohlheyer, D. A microfluidic photobioreactor for simultaneous observation and cultivation of single microalgal cells or cell aggregates. *PLoS One* **2019**, *14*, e0216093, doi:10.1371/journal.pone.0216093.
21. Alias, A.B.; Mishra, S.; Pendharkar, G.; Chen, C.; Liu, C.; Liu, Y.; Yao, D. Microfluidic Microalgae System: A Review. *Molecules* **2022**, *27*, doi:10.3390/molecules27061910.
22. Kürsten, D.; Cao, J.; Funfak, A.; Müller, P.; Köhler, J.M. Cultivation of *Chlorella vulgaris* in microfluid segments and microtoxicological determination of their sensitivity against CuCl2 in the nanoliter range. *Eng. Life Sci.* **2011**, *11*, 580–587, doi:10.1002/elsc.201100023.

23. Cao, J.; Kürsten, D.; Krause, K.; Kothe, E.; Martin, K.; Roth, M.; Köhler, J.M. Application of micro-segmented flow for two-dimensional characterization of the combinatorial effect of zinc and copper ions on metal-tolerant Streptomyces strains. *Appl. Microbiol. Biotechnol.* **2013**, *97*, 8923–8930, doi:10.1007/s00253-013-5147-8.
24. Pit, A.; Duits, M.; Mugele, F. Droplet Manipulations in Two Phase Flow Microfluidics. *Micromachines (Basel)* **2015**, *6*, 1768–1793, doi:10.3390/mi6111455.
25. Cao, J.; Kürsten, D.; Schneider, S.; Knauer, A.; Günther, P.M.; Köhler, J.M. Uncovering toxicological complexity by multi-dimensional screenings in microsegmented flow: modulation of antibiotic interference by nanoparticles. *Lab Chip* **2012**, *12*, 474–484, doi:10.1039/C1LC20584F.
26. Colin, P.-Y.; Kintses, B.; Gielen, F.; Miton, C.M.; Fischer, G.; Mohamed, M.F.; Hyvönen, M.; Morgavi, D.P.; Janssen, D.B.; Hollfelder, F. Ultrahigh-throughput discovery of promiscuous enzymes by picodroplet functional metagenomics. *Nat Commun* **2015**, *6*, 10008, doi:10.1038/ncomms10008.
27. Lemke, K.; Förster, T.; Römer, R.; Quade, M.; Wiedemeier, S.; Grodrian, A.; Gastrock, G. A modular segmented-flow platform for 3D cell cultivation. *J. Biotechnol.* **2015**, *205*, 59–69, doi:10.1016/j.jbiotec.2014.11.040.
28. Martin, K.; Henkel, T.; Baier, V.; Grodrian, A.; Schön, T.; Roth, M.; Michael Köhler, J.; Metze, J. Generation of larger numbers of separated microbial populations by cultivation in segmented-flow microdevices. *Lab Chip* **2003**, *3*, 202–207, doi:10.1039/B301258C.
29. Zheng, B.; Tice, J.D.; Ismagilov, R.F. Formation of Droplets of Alternating Composition in Microfluidic Channels and Applications to Indexing of Concentrations in Droplet-Based Assays. *Anal. Chem.* **2004**, *76*, 4977–4982, doi:10.1021/ac0495743.
30. Churski, K.; Kaminski, T.S.; Jakiela, S.; Kamysz, W.; Baranska-Rybak, W.; Weibel, D.B.; Garstecki, P. Rapid screening of antibiotic toxicity in an automated microdroplet system. *Lab Chip* **2012**, *12*, 1629–1637, doi:10.1039/C2LC21284F.
31. Cao, J.; Richter, F.; Kastl, M.; Erdmann, J.; Burgold, C.; Dittrich, D.; Schneider, S.; Köhler, J.M.; Groß, G.A. Droplet-Based Screening for the Investigation of Microbial Nonlinear Dose-Response Characteristics System, Background and Examples. *Micromachines (Basel)* **2020**, *11*, doi:10.3390/mi11060577.
32. Yu, J.; Liberton, M.; Cliften, P.F.; Head, R.D.; Jacobs, J.M.; Smith, R.D.; Koppenaal, D.W.; Brand, J.J.; Pakrasi, H.B. Synechococcus elongatus UTEX 2973, a fast growing cyanobacterial chassis for biosynthesis using light and $CO_2$. *Sci. Rep.* **2015**, *5*, 8132, doi:10.1038/srep08132.
33. Coronado-Reyes, J.A.; Salazar-Torres, J.A.; Júarez-Campos, B.; González-Hernández, J.C. *Chlorella vulgaris*, a microalgae important to be used in Biotechnology: a review. *Food Sci. Technol* **2022**, *42*, doi:10.1590/fst.37320.
34. Mangesh, B.; Sugantham, F. Effect of Light Wavelengths on Biomass Production and Pigment Enhancement of *Chlorella vulgaris* in Indoor System. *Research Journal of Biotechnology* **2019**, *14*, 111–117, doi:10.6084/M9.FIGSHARE.21120067.
35. Baidya, A.; Akter, T.; Islam, M.R.; Shah, A.K.M.A.; Hossain, M.A.; Salam, M.A.; Paul, S.I. Effect of different wavelengths of LED light on the growth, chlorophyll, β-carotene content and proximate composition of Chlorella ellipsoidea. *Heliyon* **2021**, *7*, e08525, doi:10.1016/j.heliyon.2021.e08525.
36. Yadav, P.; Singh, R.P.; Rana, S.; Joshi, D.; Kumar, D.; Bhardwaj, N.; Gupta, R.K.; Kumar, A. Mechanisms of Stress Tolerance in Cyanobacteria under Extreme Conditions. *Stresses* **2022**, *2*, 531–549, doi:10.3390/stresses2040036.

 doi:10.20944/preprints202410.0943.v1



37. Luimstra, V.M.; Schuurmans, J.M.; Verschoor, A.M.; Hellingwerf, K.J.; Huisman, J.; Matthijs, H.C.P. Blue light reduces photosynthetic efficiency of cyanobacteria through an imbalance between photosystems I and II. *Photosynth. Res.* **2018**, *138*, 177–189, doi:10.1007/s11120-018-0561-5.
38. Singh, R.P.; Yadav, P.; Kujur, R.; Pandey, K.D.; Gupta, R.K. Cyanobacteria and salinity stress tolerance. *Cyanobacterial Lifestyle and its Applications in Biotechnology*; Elsevier, 2022; pp 253–280, ISBN 9780323906340.